Author Manuscript

Author Manuscript

Author Manuscript

Author Manuscript

HHS Public Access

Author manuscript

Cogn Neurosci. Author manuscript; available in PMC 2021 July 01.

Published in final edited form as:

Cogn Neurosci. 2020 ; 11(4): 175–180. doi:10.1080/17588928.2019.1694500.

Fixed and Flexible: Dynamic Prefrontal Activations and Working Memory Capacity Relationships Vary with Memory Demand

Ashti M. Shah[1,2], **Hannah Grotzinger**[1], **Jakub Kaczmarzyk**[1], **Lindsey Powell**[1], **Meryem Yücel**[3], **John D.E. Gabrieli**[1,2], **Nicholas A. Hubbard**[1,4,*]

[1]McGovern Institute for Brain Research, Massachusetts Institute of Technology, Cambridge, MA.

[2]Department of Brain and Cognitive Sciences, Massachusetts Institute of Technology, Cambridge, MA.

[3]Neurophotonics Center, Boston University, Boston, MA.

[4]Center for Brain, Biology, and Behavior, Department of Psychology, University of Nebraska, Lincoln, NE.

Abstract

Prefrontal cortex (PFC) activation during encoding of memoranda (proactive responses) is associated with better working memory (WM) compared to reactive/retrieval-based activation. This suggests that dynamic PFC activation patterns may be fixed, based upon one's WM ability, with individuals who have greater WM ability relying more on proactive processes and individuals with lesser WM ability relying more on reactive processes. We newly tested whether this heuristic applied when challenging an individual's WM capacity. Twenty-two participants ($N = 22$) underwent functional near-infrared spectroscopy (fNIRS) during a modified Sternberg WM paradigm. We tested whether the relationship between dynamic PFC activation patterns and WM capacity changed, as a function of WM demands ($N = 14$ after quality control). Here, higher-WM capacity was associated with more proactive PFC patterns, but only when WM capacity was overloaded. Lower-WM capacity was associated with these same patterns, but only when WM demand was low. Findings are inconsistent with a purely fixed view of dynamic PFC activation patterns and suggest higher- and lower-WM-capacity individuals flexibly engage PFC processes in a fundamentally different manner, dependent upon current WM demands.

Keywords

WORKING MEMORY; PREFRONTAL CORTEX; INDIVIDUAL DIFFERENCES

Understanding variation in the limits of working memory (WM capacity) is important for understanding multiple memory systems, higher-order cognitive functions, and ecologically-relevant behaviors (Cowan et al., 2005). Individual differences in WM capacity have been linked to specific neural signatures and substrates (e.g., McNab & Klingberg, 2008).

*To whom correspondence may be addressed: Nicholas A. Hubbard, Massachusetts Institute of Technology, McGovern Institute for Brain Research, 43 Vassar St., Cambridge, MA 02139, 1-617-324-3721, nhubbard@mit.edu.

Conflicts of Interest: The authors declare no competing interests.

Author Manuscript Author Manuscript Author Manuscript Author Manuscript

Qualitatively distinct, *dynamic* prefrontal cortex (PFC) activation patterns (i.e., changes in PFC activations to different task contexts) have also been associated with measures of WM performance (response time, recognition accuracy; Braver et al., 2009; Hubbard et al., 2014; Marklund & Persson, 2012; Rypma et al., 1999). Here, we newly assessed whether relationships between dynamic PFC activation patterns and WM capacity change as a function of WM demand.

Brain imaging research suggests dynamic PFC activation patterns during WM may be largely dependent upon one's WM ability. Proactive activation patterns are reflected in increased PFC activation during earlier, preparatory phases of a task (e.g., initial presentation of memoranda) and are associated with better WM performance (Braver et al., 2009; Hubbard et al., 2014). Reactive activation patterns are reflected in increased PFC activation in response to action cues (e.g., a retrieval cue), and are associated with worse WM performance (Braver et al., 2009; Hubbard et al., 2014; Rypma & D'Esposito, 2000; Rypma et al., 1999). These findings provide a useful heuristic suggesting that, during WM, proactive activation patterns are associated with better memory, whereas reactive activation patterns are generally associated with worse memory. However, this heuristic might not generalize to more nuanced task contexts (Burgess and Braver, 2010). For instance, higher-WM-capacity individuals may achieve this distinction through employing proactive cognitive strategies, such as chunking, when the demands placed upon WM are high (Hubbard et al., 2014). However, this same strategy-engagement is probably not necessary or efficient for higher-WM-capacity individuals when WM demand is low (Braver, 2012).

Here, functional near-infrared spectroscopy (fNIRS) was used to assess dynamic dorsolateral PFC activation patterns during WM performance. We examined correlations between proactive and reactive dorsolateral PFC activation differences (hereafter, P-R differences) and an individual's WM capacity. We tested whether these correlations changed when participants attempted to remember subcapacity, capacity, and supracapacity lists of letters. Importantly, P-R differences were isolated while sizes of to-be-remembered lists were calibrated to participants' WM capacities. The purpose of a priori task calibration was to isolate brain responses irrespective of influence from ongoing WM performance differences or biased-levels of task difficulty (Hillary et al., 2006).

Method

Participants

Twenty-two participants (N=22; M_{age}=37.2 y/o; SD=15.56; 95% Male). The high male-to-female ratio is probable because participants were recruited with hair less than three-inches long to strengthen the fNIRS signal (McIntosh et al., 2010). Eighty-six percent of participants were right handed, 95% were native or excellent English speakers, every participant had at least a high school education, and participants' average Montreal Cognitive Assessment score was 27.4 (SD = 2.26; indicating, on average, normal cognitive functioning). Right and left-handed participants did not show significant differences in key fNIRS or WM measures. Participants reported no history of brain injury or mental illness.

Author Manuscript Author Manuscript Author Manuscript Author Manuscript

Delayed-Response WM Tasks

Two verbal, Sternberg-type WM tasks (Sternberg, 1966) were administered using automated presentation software. The first task estimated participants' WM capacities (*K* score) and was completed before fNIRS imaging. The *K* score derived from this first WM task was used as an index of an individual's WM capacity and was used to calibrate the list-size conditions on the second WM task, which was completed during fNIRS scanning.

Pre-fNIRS WM task.—Participants remembered lists of (3 to 7) letters over an 8-s delay (see Figure 1A). Each list size was presented 7 times (35 trials total). WM capacity was estimated by adapting a standard formula (Cowan, 2001; Supplemental). Here, $K = S(H\text{-}FA)$; where *S* was the largest list size that the participant achieved with > 50% accuracy, *H* reflected correct detections (i.e., hits), *FA* reflected false detections (i.e., false alarms). Two participants failed to meet the a priori performance criterion on this task ($K<3$); their data were excluded from analyses.

fNIRS WM task.—This task was similar to the first WM task, except: (1) 10 trials were added to this task to enhance the reliability of the fNIRS signal (total trials = 45); (2) to-be-remembered list sizes were calibrated to 2 letters (subcapacity), *K* letters (capacity), and *K* +1 letters (supracapacity); (3) these calibrated-list sizes were presented 15 times each; (4) inter-trial intervals were jittered at 9, 10, or 11 seconds to accommodate hemodynamic responses; and (5) the task was broken into two ~10 min runs (total time 20 min). The 2-letter condition was held constant across participants to offer a low-load, easily achievable, subcapacity WM condition.

fNIRS Acquisition and Processing

WM-related brain activation was measured by assessing changes in oxyhemoglobin concentrations. Data were collected using CW6 NIRS laser diodes with emittance of 690 nm and 830 nm continuous wavelengths (TechEn Inc, MA, USA). fNIRS data were processed using HOMER2 software similar to extant reports (Jahani et al., 2017; Supplemental). Unreliable and noisy channels were filtered). Filtering decisions were based upon aggregate task responses which did not take into account list size or WM phase conditions; thus, did not bias hemoglobin estimates for any experimental condition of interest (i.e., list size or WM phase differences; Figure 2C; Supplemental). Six out of 20 participants did not demonstrate at least one reliable channel across runs; their data were not used in subsequent analyses.

Event-related fNIRS Activations.—Homer2's ordinary-least-squares general linear models (GLM; Ye et al., 2009) examined task-versus-rest activations for the three different WM list size conditions (i.e., 2, *K*, *K*+1) × three different WM phases (i.e., encode, delay, retrieval cue) on hemoglobin concentration data. This yielded a 3×3 design matrix for explanatory factors which also included additional nuisance regressors (detailed below). Homer2's modified-gamma impulse response functions, t_{step}=.02 s; t_{range}=0–16 s, were applied to the design matrix to model demand and phase effects. Gamma functions were used because our previous work using the Sternberg task during fMRI used gamma-based canonical models to demonstrate P-R differences in group analyses (Hubbard et al., 2014).

Author Manuscript Author Manuscript Author Manuscript Author Manuscript

The modified-gamma approach applied by Homer2 convolves a gamma basis function with a square-wave function of duration T, where $T = 16$ s here to allow for statistical independence between modeled hemodynamic responses from each condition onset (Rypma and D'Esposito, 2000). Third-order signal drifts and signals from short-separation channel within a maximum distance of 10 mm of a given optode were added as nuisance factors in these GLMs to control for potential non-neural effects (e.g., biological motion, general changes in superficial hemodynamics), and yield more accurate cortical hemodynamic estimates (Gagnon et al., 2011). GLMs produced a modeled time course of hemoglobin changes from baseline, statistically independent of nuisance factors and other individual task conditions. The sum of oxyhemoglobin concentrations (i.e., area-under-the-curve of the gamma-response function [Jahani et al., 2017]) within this time course was averaged across all channels surviving filtering. This provided a single, aggregate measure of dorsolateral PFC oxyhemoglobin concentration at each list-size condition × encoding or retrieval phases. We focused these analyses upon P-R differences, operationalized as encoding subtracted from retrieval oxyhemoglobin concentrations (Hubbard et al., 2014). Contrasting WM phases within participants would eliminate biases associated with increased activation in experimental conditions—which might be expected because individuals with higher-K scores were given larger lists during capacity and supracapacity conditions, relative to individuals with lower-K scores.

Results

Performance

Pre-fNIRS WM task.—Accuracy and response times (RT) demonstrated expected patterns with increasing list size (Figure 1B). Median K was 6 (MAD=1; Range=4–7) and the distribution of K-scores for the 14 participants retained in these analyses was: K_4= 7.14% (1); K_5= 21.42% (3); K_6= 42.86% (6); K_7= 28.57% (4).

fNIRS WM task.—Accuracy and RT demonstrated expected patterns across calibrated-list size conditions (Figure 2A). There were no significant relationships found between recognition accuracy and individual differences in K derived from the pre-fNIRS task, at any list size (ps > .10), indicating calibration mitigated the effects of ability on ongoing recognition accuracy on the fNIRS WM task. K scores were significantly related to K-letters and K+1-letters RTs (Spearman's $\rho(12)$=.67 and $\rho(12)$=.56, respectively; ps < .05), but not the 2-letter condition (p > .35).

WM Capacity and Dynamic PFC Relationships Vary with Calibrated List Size

Hypothesis testing focused upon the extent to which P-R differences, operationalized as encoding subtracted from retrieval oxyhemoglobin concentrations (Hubbard et al., 2014), were related to individual differences in K scores. Contrasting WM phases within participants served to eliminate biases associated with increased activation in experimental conditions—which might be expected because individuals with higher-K scores were given larger lists during capacity and supracapacity conditions, relative to individuals with lower-K scores. These hypothesis tests were exploratory, thus, false-discovery-rate corrections were

Author Manuscript Author Manuscript Author Manuscript Author Manuscript

applied to limit the probability of Type-I error when examining their correlations to behavior (Hochberg and Benjamini, 1990).

K scores had a significant, positive relationship with P-R differences at supracapacity list sizes ($\rho(12)=.68$; FDR-corrected $p<.05$; BCa-bootstrap $CI_{95\%}= .23 – .89$). A significant, negative relationship was observed at the subcapacity list size ($\rho(12)= -.64$; FDR-corrected $p<.05$; BCa-bootstrap $CI_{95\%}= -.09 - -.93$). Fisher's *z*-test revealed that correlations between *K* scores and P-R differences for supracapacity and subcapacity list sizes were significantly different ($z(14) = 3.98$; $p < .001$). No significant relationship was observed when list size matched individuals' *K* scores ($\rho(12)=.18$; FDR-corrected $p>.05$; BCa-bootstrap $CI_{95\%}= -.60 – .81$;see Figure 3).

Calibration was successful in mitigating potential performance or task-demand confounds on P-R differences. No significant correlations were observed between recognition accuracy on the fNIRS WM task and P-R differences (all list conditions: *p*s>.05). No significant correlations were observed between recognition RT and P-R differences during 2 or *K*-item list sizes (all *p*s>.05). There was a significant relationship observed between P-R differences and recognition RT at *K*+1 items list size ($\rho(12)=.53$, uncorrected $p = .051$). This relationship failed to reach significance after FDR correction (FDR-corrected $p = .15$) and it was influenced by the relationship between WM capacity estimates and *K*+1 items recognition RT (see above). The relationship between *K*+1 items recognition RT and P-R differences was not significant when partialing the variance accounted for our behavioral variable of interest, *K* scores ($r(11)_{XY|Z} = .13$, $p > .67$).

Discussion

The novel finding in the present report was that the correlation between WM capacity and dynamic PFC activations changed under different WM-demand conditions. From previous brain imaging studies of WM, a heuristic could be suggested: greater WM ability is associated with a tendency to engage proactive PFC responses, and lesser WM ability is associated with a tendency to engage reactive responses (Braver et al., 2009; Hubbard et al., 2014; Rypma & D'Esposito, 2000; Rypma et al., 1999). It has also been posited that lower-WM capacity individuals primarily rely upon automatic (i.e., reactive), as opposed to more premeditated or controlled (i.e., proactive) PFC-mediated processes (Kane and Engle, 2002). Here, both higher- and lower-*K* scores were associated with greater encoding relative to retrieval dorsolateral PFC activation (i.e., proactive activation pattern). However, the tendency to emphasize a proactive or reactive activation pattern, changed as a function of both WM capacity and the demands placed upon an individual's WM.

Findings suggest similar engagement of PFC-mediated cognitive processes between higher- and lower-WM-capacity individuals, but, under different circumstances. Proactive cognitive processes may reflect attentional biases toward goal-relevant material or the recruitment of mnemonic strategies (Braver et al., 2009; Hubbard et al., 2014). When WM demands are low, higher-WM-capacity individuals might not perceive advantage in engaging proactive cognitive processes and rely upon their superior storage capacity alone, whereas, for lower-WM-capacity individuals, such processes might be required for encoding even low volumes

Author Manuscript Author Manuscript Author Manuscript Author Manuscript

of information (Kane et al., 2007). Conversely, when WM demand exceeds one's immediate storage capacity, higher-WM-capacity individuals may attempt to manage this larger volume of information using proactive cognitive processes. However, lower-WM-capacity individuals may be unwilling or unable to use these processes past their peak, potentially because they perceive a low probability of those processes being successful (Braver, 2012). Thus, under supracapacity WM conditions, lower-WM-capacity individuals rely upon reactive, PFC-based processing mechanisms; possibly reflecting late attempts to reactivate encoded memory patterns or later use of attention to attempt to circumvent retrieval interference (Braver et al., 2009; Sprague et al., 2016).

A limitation of this study was that results were derived from a relatively small and homogenous participant sample. Statistical analyses were therefore relatively conservative. Tests were exploratory and FDR corrections reduced the probability of Type-I error. The use of nonparametric correlations also circumvented assumptions of normality within our sample, which are often violated in smaller samples. Although these statistical approaches increase confidence in the generalizability of the present findings, future research is needed for further confirmation of these findings.

The present findings do offer preliminary evidence that dynamic PFC activation patterns during WM may be both fixed and flexible. On the one hand, dynamic PFC patterns may be fixed in the sense that such patterns are in fact related to one's WM ability (e.g., capacity). On the other hand, these patterns may also be flexible in the sense that they vary depending upon current demands placed upon one's WM. The more flexible aspect of dynamic PFC activation patterns is consistent with the presumed function of PFC as a hub for adaptively modulating neural responses in the service of ever-changing, contextually-relevant demands (Miller and Cohen, 2001). Conversely, the relationships observed between WM capacity and dynamic PFC activation patterns also suggest one's WM ability is intimately related to the manner in which PFC responds, even given similar contexts (e.g., calibrated demand conditions [Rypma and D'Esposito, 1999]). Interestingly, together these findings imply that a heuristic hypothesis regarding the role of dynamic PFC activations (proactive = greater WM ability; reactive = lesser WM ability) might not be generalizable to differing demand contexts and they implore novel exploration of mediators (e.g., reward signals from subjective-valuation regions [Westbrook et al., 2019]) driving the relationship between WM ability and dynamic PFC activations.

Supplementary Material

Refer to Web version on PubMed Central for supplementary material.

Acknowledgements:

This work was supported in part by a Johnson and Johnson Women in STEM fellowship to AMS and National Institutes of Health grants to NAH (F32MH114525).

References

Aasted CM et al. (2015). Anatomical guidance for functional near-infrared spectroscopy: AtlasViewer tutorial. Neurophotonics, 2(2), 020801. [PubMed: 26157991]

Author Manuscript Author Manuscript Author Manuscript Author Manuscript

Braver TS et al. (2009). Flexible neural mechanisms of cognitive control within human prefrontal cortex. PNAS, 106(18), 7351–7356. [PubMed: 19380750]

Braver TS (2012). The variable nature of cognitive control: a dual-mechanisms framework. TICS, 16(2), 106–113.

Burgess GC, Braver TS (2010). Neural mechanisms of interference control in working memory: Effects of interference expectancy and fluid intelligence. PLoS One, 5(9), e12861. [PubMed: 20877464]

Cowan N (2001). The magical number 4 in short-term memory: A reconsideration of mental storage capacity. Behav Brain Sci, 24(1), 87–114. [PubMed: 11515286]

Cowan N et al. (2005). On the capacity of attention: Its estimation and its role in working memory and cognitive aptitudes. Cogn Psychol, 51(1), 42–100. [PubMed: 16039935]

Hillary FG et al. (2006). Prefrontal modulation of working memory performance in brain injury and disease. Hum Brain Mapp, 27(11), 837–847. [PubMed: 16447183]

Hubbard NA et al. (2014). Central executive dysfunction and deferred prefrontal processing in veterans with Gulf War Illness. Clin Psychol Sci, 2(3), 319–327. [PubMed: 25767746]

Jahani S et al. (2017). fNIRS can robustly measure brain activity during memory encoding and retrieval in healthy subjects. Sci Reports, 7(1), 9533.

Kane MJ, Engle RW (2002). The role of prefrontal cortex in working memory capacity, executive attention, and general fluid intelligence: An individual-differences perspective. Psychonom Bul Rev, 9(4), 637–671.

Kane MJ et al. (2007). For whom the mind wanders: An experience-sampling study of working memory and executive control in daily life. Psychol Sci, 18(7), 614–621. [PubMed: 17614870]

Marklund P, Presson J (2012). Context-dependent switching between proactive and reactive working memory control mechanisms in the right inferior frontal gyrus. NeuroImage, 63(3), 1552–1560. [PubMed: 22906785]

McIntosh MA et al. (2010). Absolute quantification of oxygenated hemoglobin within the visual cortex with functional near infrared spectroscopy (fNIRS). Invest Opthalmol Visual Sci, 51(9), 4856–4860.

McNab F, Klingberg T (2008). Prefrontal cortex and basal ganglia control access to working memory. Nat Neurosci, 11(1), 103–107. [PubMed: 18066057]

Miller EK, Cohen JD (2001). An integrative theory of prefrontal cortex function. Ann Rev Neurosci, 24, 167–202. [PubMed: 11283309]

Powell LJ et al. (2018). Using individual functional channels of interest to study cortical development with fNIRS. Dev Sci, 21(4), e12595. [PubMed: 28944612]

Rypma B et al. (1999). Load-dependent roles of frontal brain regions in the maintenance of working memory. NeuroImage, 9(2), 216–226. [PubMed: 9927550]

Rypma B, D'Esposito M (1999). The roles of prefrontal brain regions in components of working memory: Effects of memory load and individual differences. PNAS, 96, 6558–6563. [PubMed: 10339627]

Rypma B, D'Esposito M (2000). Isolating the neural mechanisms of age-related changes in human working memory. Nat Neurosci, 11(1), 509–515.

Sprague TC et al. (2016). Restoring latent visual working memory representations in human cortex. Neuron, 91(3), 694–707. [PubMed: 27497224]

Sternberg S (1966). High-speed scanning in human memory. Science, 153, 652–654. [PubMed: 5939936]

Westbrook A, Lamichhane B, Braver T (2019). The subjective value of cognitive effort is encoded by a domain-general valuation network. J Neurosci, 39(20), 3934–3947. [PubMed: 30850512]

Author Manuscript Author Manuscript Author Manuscript Author Manuscript

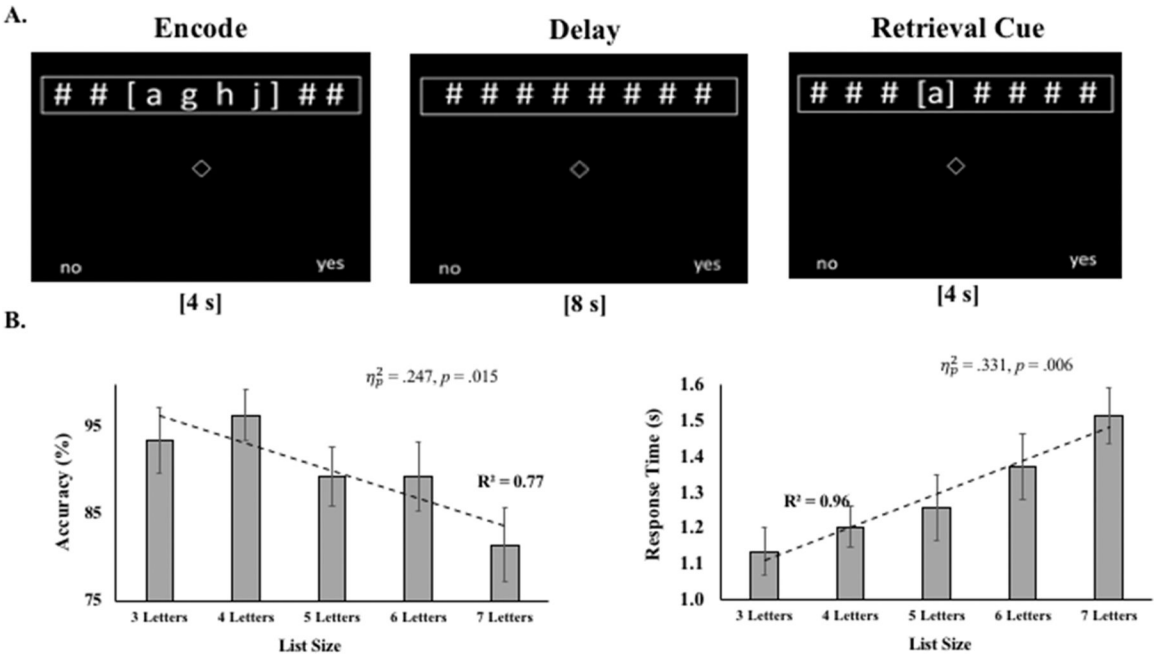

Figure 1. Task Example and Performance on the Pre-fNIRS WM Task.

A. Example of a single trial of the Sternberg-type working memory tasks. Varying sizes of lists were presented for four seconds. Participants were required to remember lists over an 8 second delay. Then, participants responded “yes” or “no”, via “z” or “/” computer keys, regarding whether a retrieval-cue letter matched one in the to-be-remembered list. Accurate “yes” and “no” responses were balanced. Perceptual load was balanced across task epochs. List sizes were presented pseudo-randomly. **B.** Accuracy and response time as a function of list size on the *pre*-fNIRS WM task. Group means and one standard error of the mean. Dotted line = OLS regression line. R^2 = OLS fit. Partial-eta-squared = effect size from repeated measures ANOVAs.

Author Manuscript
Author Manuscript
Author Manuscript
Author Manuscript

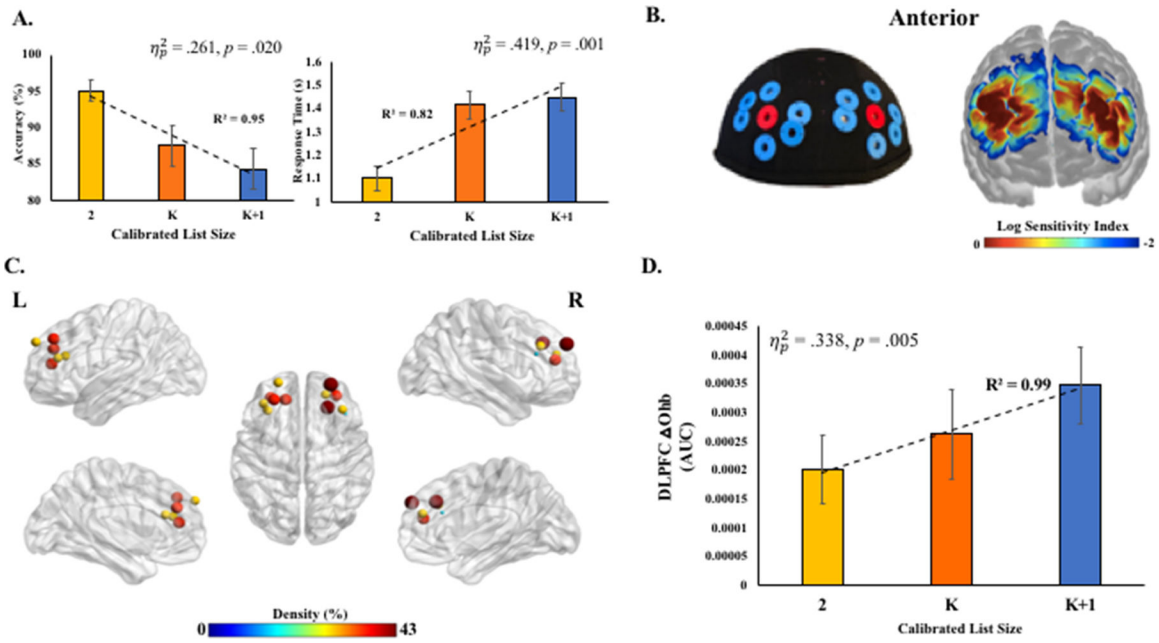

Figure 2.

A. Accuracy and response time as a function of calibrated list size on the fNIRS WM task. **B.** fNIRS probe configuration on cap and sensitivity index via Monte Carlo simulations of photon migration. Log sensitivity index values closer to zero reflect greater sensitivity for acquiring signals in that region (see Aasted et al., 2015). Two short- (7.5 mm from source [red grommets]) and 12 standard-separation (30 mm from source [blue grommets]) channels were placed in standardized space, and centered around left and right dorsolateral PFCs (F4 and F3 in 10–20 system) using AtlasViewer software (Aasted et al., 2015), MNI-space coordinates may be found in Supplemental Table 1. Localization of dorsolateral PFC on individual participants was achieved by land marking inion and nasion, and then securing the cap which was standardized to 10–20 landmarks surrounding bilateral dorsolateral PFCs. **C.** Post-filtering channel density. Size and color of nodes reflect the percent of participants retained after filtering for a given channel. **D.** Proof-of-principle hypothesis test (Supplemental; pre-registered at osf.io/hzvp9/). DLPFC aggregate oxyhemoglobin concentrations (area-under-the-curve [AUC]) from post-filtering channels increased with calibrated list size. Group mean and one standard error of the mean.

Author Manuscript Author Manuscript Author Manuscript Author Manuscript

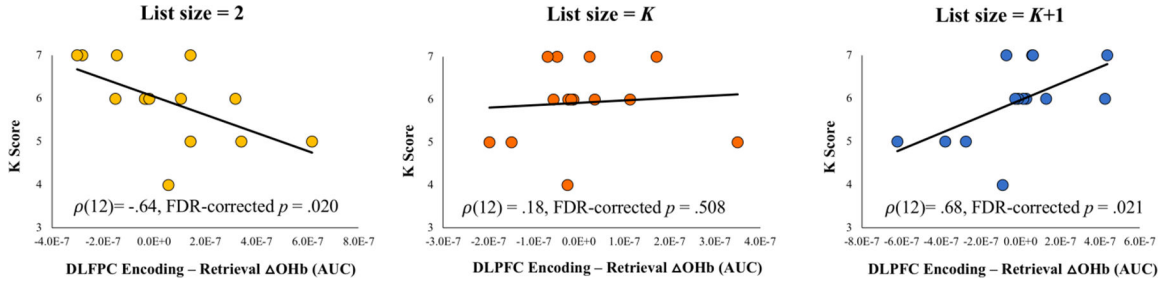

Figure 3.

A. Working memory capacity (*K* score) derived from the pre-scan WM task and P-R differences (encoding minus retrieval) in DLPFC oxyhemoglobin concentrations (area-under-the-curve) across the three, calibrated list-size conditions. ρ = Spearman's rho was used as a nonparametric estimation of the relationship between capacity and P-R differences in DLPFC activation. Nonparametric tests were used because *K* distributions are based upon discrete values. *p*-values were adjusted for false discovery rate on the number of comparisons of the list size condition.